

Evaluation of the mechanical performance of iron – polymethyl methacrylate and polystyrene polymer products based on alumina nanomaterials

Muzher Taha Mohamed¹, Sami A. Nawi¹, Hiba M. Algailani², Ahmed A.A.G. Alrubaiy¹, Adel K. Mahmoud¹, Salem Farman³, Ali Mundher Mustafa^{4*} , A.A. Alamiery⁵

¹ Bilad Alrafidain University College, Diyala, Iraq

² Department of Materials Engineering, College of Engineering, University, of Diyala, Iraq

³ Department of Refrigeration and Air Conditioning, College of Technical Engineering, Al- Farahidi University

⁴ Production Engineering and Metallurgy, University of Technology, Baghdad, Iraq

⁵ Biomedical Engineering Department, College of Engineering, Al-Ayen University (AUIQ), Nasiriyah, Iraq

* Corresponding author's e-mail: ali.m.mustafa@uotechnology.edu.iq

ABSTRACT

In this investigation, alumina (Al_2O_3) nanoparticles were utilized to study the mechanical properties of two polymer nanocomposite systems applied to low-carbon steel substrates. The nanocomposites comprised polystyrene (PS) and polymethylmethacrylate (PMMA) matrices, each incorporating 5 wt.% Al_2O_3 nanoparticles. Tensile tests revealed that the nanocomposites exhibited superior mechanical performance compared to pure polymers. For PMMA- Al_2O_3 , tensile properties such as elastic modulus (E), ultimate tensile strength (σ_{ult}), and strain (ϵ_{ult}) were 2.6326 GPa, 44.52 MPa, and 0.02560, respectively, showing improvements of 16.5% in σ_{ult} and 33.7% in ϵ_{ult} . Similarly, PS- Al_2O_3 showed σ_{ult} and ϵ_{ult} improvements of 19.1% and 61.5%, respectively, compared to pure PS. The Scanning electron microscopy (SEM) revealed flocculation and uneven nanoparticle dispersion. At low magnification (1.56 μm), PS- Al_2O_3 particles were well-separated, while higher magnification (11.6 μm) showed aggregation. The average nanoparticle diameters for PMMA- Al_2O_3 and PS- Al_2O_3 were 201.1 nm and 184.6 nm, respectively. Flocculation and low-density interphase, attributed to fewer polymer chain anchoring sites on Al_2O_3 surfaces, reduced the elastic modulus. These findings emphasize the need for advanced blending techniques to achieve uniform nanoparticle distribution and improve polymer-nanoparticle interfacial bonding. Optimized dispersion methods are crucial for enhancing the mechanical properties of Al_2O_3 -reinforced nanocomposites.

Keywords: polymethyl methacrylate (PMMA), polystyrene (PS), aluminum oxide (Al_2O_3), mechanical properties, SEM.

INTRODUCTION

PMMA and PS are widely used in biomedical and industrial applications due to their excellent mechanical properties, biocompatibility, and ease of processing. However, their inherent limitations, such as brittleness and low impact resistance, necessitate modifications to meet the demands of advanced applications. One promising approach is the incorporation of nanoparticles like alumina (Al_2O_3), which can enhance their mechanical, thermal, and tribological properties by reinforcing the polymer matrix.

Theoretical studies have shown that nanoparticle reinforcement can improve material strength, toughness, and overall performance through mechanisms such as load transfer, crack deflection, and barrier effects. However, achieving uniform dispersion and strong interfacial bonding between nanoparticles and polymer chains remains a significant challenge. Poor dispersion can lead to agglomeration, limiting the effectiveness of the reinforcement and creating weak zones in the material.

This study investigates the mechanical properties of PMMA and PS nanocomposites

reinforced with Al₂O₃ nanoparticles. The problem lies in understanding how processing techniques affect nanoparticle dispersion, interphase density, and the overall enhancement of the composite's properties. Previous research has highlighted the influence of nanoparticle concentration on properties such as tensile strength, hardness, and impact resistance. Awate and Barve [12] demonstrated that optimal nanoparticle concentration (e.g., 4 wt.%) could significantly improve tensile strength in metal matrix composites. Similarly, Aghajani Derazkola and Simchi [13] observed that increasing nanoparticle volume fraction in PMMA enhanced mechanical properties but led to agglomeration at higher concentrations.

Studies by Mohmoudian et al. [14], Gallab et al. [15], and Ash et al. [16] emphasized the role of nanoparticle size, dispersion, and interfacial bonding in determining mechanical performance. For instance, Gallab et al. [15] reported a 14.7% increase in hardness and a 0.27% improvement in fracture toughness for PMMA with 0.6 wt.% Al₂O₃ [17–18]. Despite these advancements, issues like agglomeration and low-density interphases persist [19–20].

Aim of the study

The study aimed to evaluate the mechanical properties and microstructural characteristics of PMMA and PS polymer nanocomposites, each reinforced with 5 wt.% Al₂O₃ nanoparticles and applied to low-carbon steel substrates. It focused on determining the impact of Al₂O₃ addition on tensile properties, elastic modulus, ultimate tensile strength, strain and nanoparticle dispersion within the matrices.

Importance of research results

Enhanced mechanical performance – Al₂O₃ nanoparticles significantly improved tensile strength, elasticity, and strain capacity in both PMMA and PS, broadening their applicability in demanding environments. Microstructural Insights: SEM analysis highlighted dispersion challenges and flocculation, providing valuable information on optimizing nanoparticle distribution to improve performance.

Practical applications – findings support the use of Al₂O₃-reinforced polymers in biomedical, structural, and industrial fields requiring materials with superior strength and toughness.

Motivation for selecting the materials

PMMA and PS – chosen for their versatile applications and potential for enhancement through nanoparticle reinforcement. Al₂O₃ Nanoparticles selected for their exceptional hardness, thermal stability, and proven effectiveness in improving polymer mechanical properties. Application potential – motivated by the demand for durable, flexible materials in structural and biomedical applications.

EXPERIMENTAL WORKS

The initial system blending

Four polymer nanocomposite systems (PS-Al₂O₃ and PMMA-Al₂O₃, each with 5 wt.% alumina) and two pure reference polymers (PS and PMMA) were prepared on low-carbon steel (AISI 1020) substrates. The number of specimens for each system produced enough samples for mechanical and microstructural analyses. Specifically, 10 specimens per group were tested for tensile strength, elastic modulus, and strain. Then the sample preparation were start at nanocomposite preparation – a solution containing 15 wt.% polymer and 5 wt.% alumina nanoparticles was synthesized for each nanocomposite system, while the reference polymers used a 30 wt.% polymer solution.

PS-based system dissolved in toluene with controlled stirring and heating at 60 °C to 80 °C until a homogeneous solution was achieved (approximately 3 hours). Then the PMMA-based system dissolved in chlorobenzene with adjusted temperatures and dissolution times to optimize polymer dissolution and nanoparticle distribution.

Table 1 provides the element levels utilized to synthesize primary mixtures. Erlenmeyer flasks hold all samples. Before using flasks, stirrers, spatulas, slides, and other lab equipment, they have been washed by water and Alconox soap, then rinsed by acetone, then rinsed by proper solvent, and finally dried in a Fisher scientific isothermal dehydrated furnace at 100 °C for 20 min.

Aldrich Chemical Company, Inc. supplied PS pellets and PMMA granules with MW = 400,000 g/mol and 1.032 and 1.210 g/cc densities, respectively. The current alumina study used 4 g/cc PMMA and 20 nm nanoparticles. Toluene (0.867 g/cc, Fisher scientific) dissolved all polystyrene-based systems. Chlorobenzene, with a density of 1.106 g/cc at 99% purity, is the solvent for the poly (methyl methacrylate)-based system.

Table 1. Polymer nano-composite system constituents

System	Polymer-Matrix (ml)	Second phase (Filler) (g)	Solvent (ml)
PMMA (Pure/Reference)	32.48	–	110
PMMA - Al ₂ O ₃	30	0.5	203
PS (pure/reference)	36.34	–	140
PS - Al ₂ O ₃	40	0.5	309

The sample preparation for all systems was the same. PS-Al₂O₃ samples were prepared using a stirrer, a spatula, a volumetric cylinder, and a 1000-ml that have been setup. The flask received 385 ml of toluene. The flask is on a 60 °C, 500 rpm Thermocline Miraka mixing hot-plate. The flask contains a spinning magnetic stirrer and toluene and 50 grams of PS. PS initially developed a sticky layer at the flask’s bottom. The flask reached a temperature of 80 °C. Beyond 3 hr the mix became unpoluted, and the stirrer was freely spinning, showing the dissolution of polymer. Mass of 500 milligrams of magnetite were weighed. For 10 minutes, the flask mixes the alumina (Al₂O₃) while the circulating the mixture. A fume hood covers the flask with a canning parafilm “M” laboratory film. PMMA-Al₂O₃ was made using the same method, but with different temperatures and dissolution times. The synthesized solutions were used to make all testing samples.

Inspection and testing

Tensile test

Tensile testing samples require special preparation. Despite the changes to improve the sample quality, six systems’ samples were made using the same processes. Also, pre-mixed tensile test samples were made as a “dog bone” shape. The sample’s construction focused on removing the solvents and preventing the neck air pockets. Each system has many samples.

Four ASTM D638-compliant aluminum molds were produced. The 18 cm × 5 cm × 2 cm molds feature the replaceable top, bottom, and center sections. To remove a hardened sample, the molds have slots on the top and bottom. Before applying the mold, spray on dry film was sprayed on the all sample-contact regions. The mold release agent made removing the hardened samples easier.

Beyond two days, the solvent has evaporated in the dehydrated furnace, as well as all samples have been vacuum-dried. They were warmed

in a prepared vacuum furnace at 100–120 °C for an hour. The mold was kept in the 1500 kPa vacuum furnace. Then, tensile test samples were solvent-free. After removing the mold from the furnace, the sample was repressed while warming to reduce air bubbles and improve layer bonding. Slowly, all mold samples were then removed. All the sample edges were smoothed using emery papers. A 0.1-micrometer was used to measure the dimensions of all samples. Magnetite and aluminum samples were dark brown and slightly transparent pale yellow.

Tensile test equipment (WDW-200e) available in the Department of Materials Engineering/University of Technology in Baghdad, was used for testing the all materials. It is computerized and has a capacity of 20 kN. Extensometers were used for measuring the strain. The machine and extensometer were calibrated before use. A two-sided tape has been twisted over the sample where the extensometer has been placed, as well as elastic strong rubber bands have been utilized for tightening every end for preventing the sliding.

Scanning electron microscopy

Scanning electron microscopy (SEM) was employed to analyze the tensile test sample’s particle distribution and size. Carbon tape under the sample and a little roll around were used to stabilize it upon the holder of sample. Also, polymers being non-conductive as well as may be charged in this device; hence all samples have been sputtered to be coated by gold. The samples’ tiny gold-atom coating eliminated the charging. The samples were sputtered to be coated for 90 seconds in a 100 kPa sputter coater chamber to reduce the gold layer thickness and the surface distortion. TScan Vega 3 SEM was used at 30 kV. Each sample was photographed using Vega 3 processed images. The software measured the particle size.

RESULTS AND DISCUSSION

Results of tensile test

These tests have been performed for assessing the polymer nano-composites' mechanical characteristics. Several factors influence the polymers' mechanical properties, including history of processing, molecular weight, and tacticity. As a result, the reference systems of pure polymer, which may be directly compared to the nano-composites, have been studied.

Device of the tensile test was used to measure the extension resistance load of sample. And, the experimental tensile test was conducted at a (2 mm/min) cross-head speed. The load extension curves of PMMA and PS are shown in Figures 1 and 2, respectively. The engineering stress-strain curves of polymethyl methacrylate (PMMA) and

polystyrene (PS) are depicted in Figures 3 and 4, respectively. Figures 5 and 6 show PMMA and PS true stress-strain curves. Table 2 for PMMA and Table 3 for PS show the computed tensile characteristics. Both reference systems have higher moduli of elasticity than the additive system. Al_2O_3 also increases the maximum tensile strength. Table 4 shows maximum tensile strength and strain percentage changes. Al_2O_3 increases the ultimate strain (ϵ_{ult}), maximum tensile stress, and percent elongation (ϵ). Al_2O_3 improved both groups' performance over PS and PMMA, respectively. This results are agreement with others studies [13, 15, 16].

Scanning electron microscopy

The scanning electron microscope was utilized to analyze particle size and dispersion, focusing on

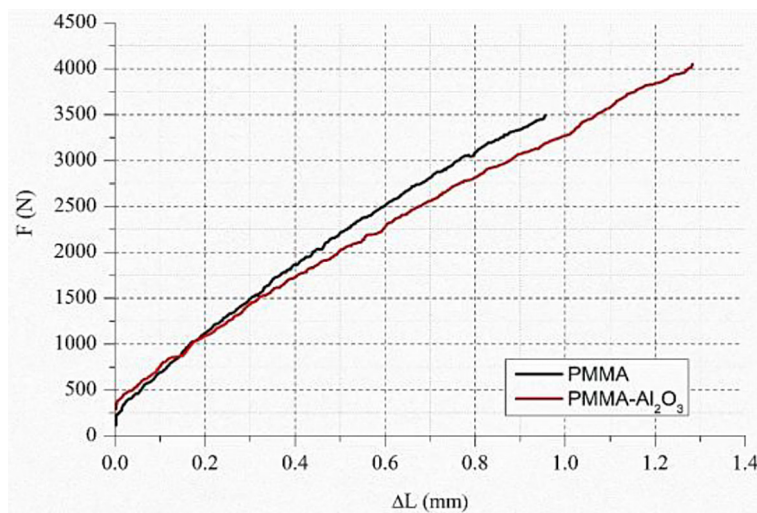


Figure 1. PMMA group load-extension curves

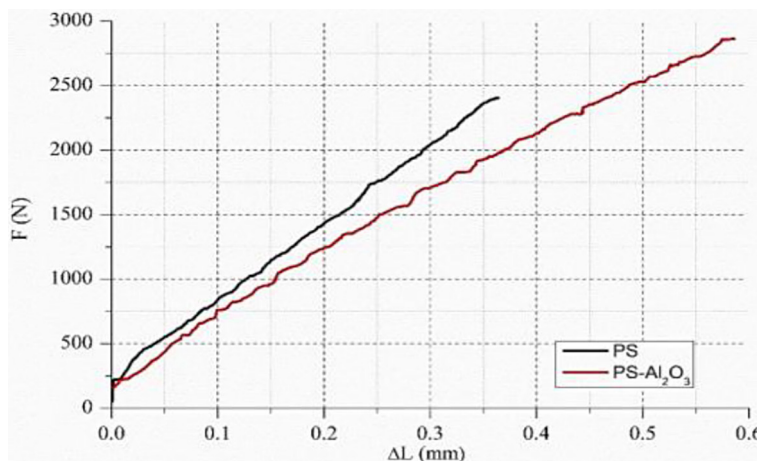


Figure 2. PS group load-extension curve

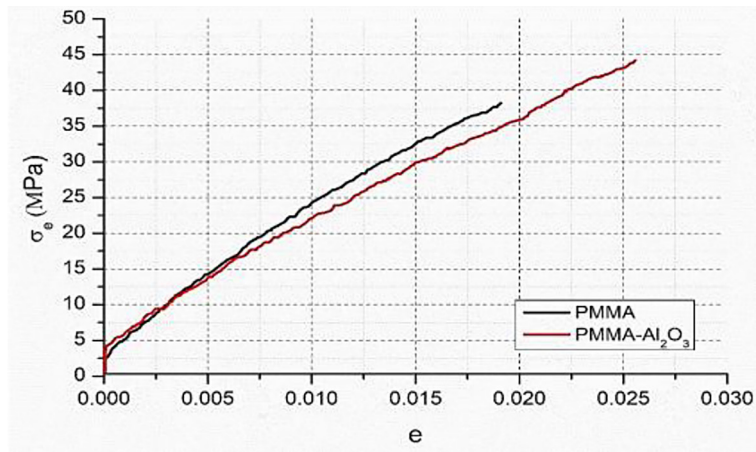


Figure 3. PMMA group engineering stress-strain curves

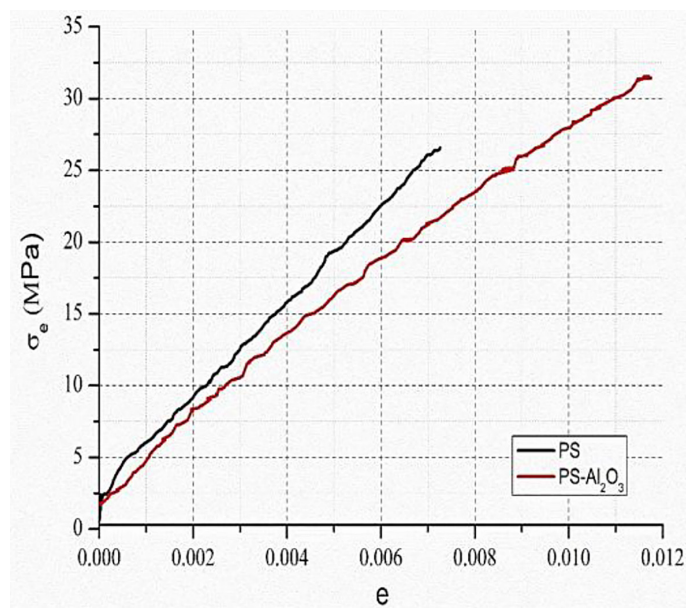


Figure 4. PS group engineering stress-strain curves

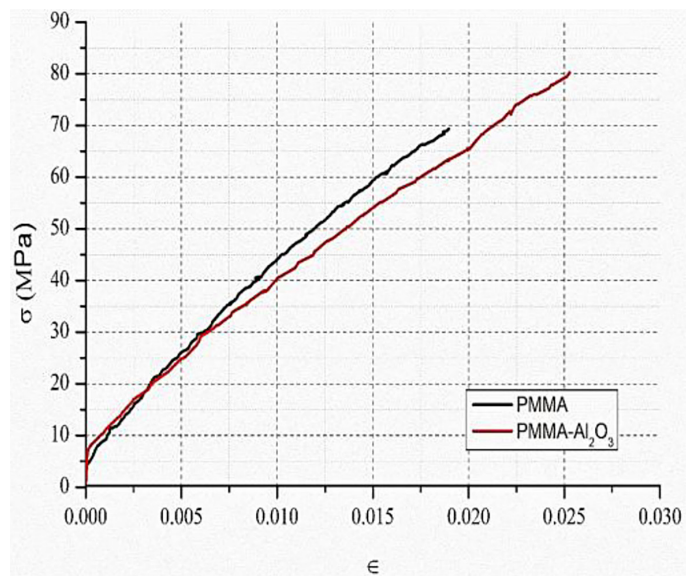


Figure 5. PMMA group true stress-strain curves

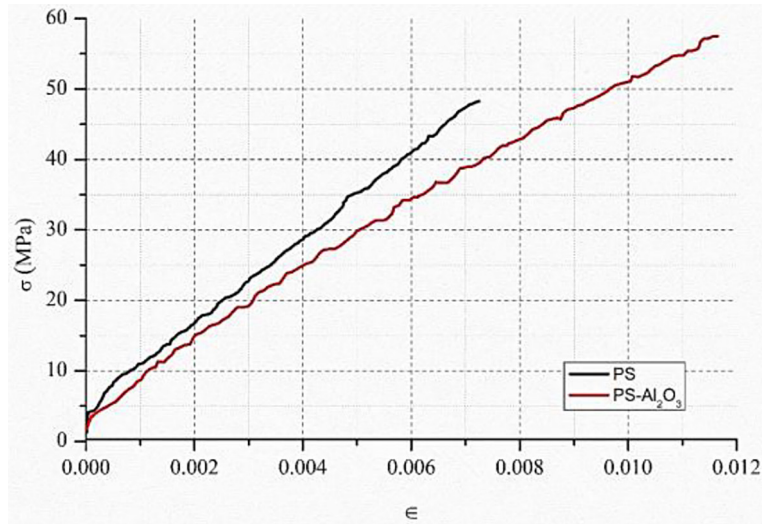


Figure 6. PS group true stress-strain curves

Table 2. PMMA group tensile test results

System	E (GPa)	σ_{ult} (MPa)	σ_y (MPa)	e_{ult}	e %
PMMA	2.8103	38.22	13.69	0.01915	1.9146
PMMA- Al_2O_3	2.6326	44.52	12.6	0.02560	2.650

the interphase regions of all four nano-composite systems. For this investigation, tensile test specimen fracture surfaces were photographed using SEM to assess the dispersion and fracture characteristics. Prior to imaging, these surfaces were sputtered with a thin layer of gold atoms to mitigate charging effects, ensuring that the image quality remained unaffected during the analysis.

Figures 7–12 illustrate the SEM micrographs depicting particle dispersion within the composites. The images reveal that particle dispersion is uneven across the fracture surfaces, with notable instances of large flocculants. For instance, Figure 7 highlights a significant flocculate observed on the PMMA- Al_2O_3 composite fracture surface

under lower magnification (11.6 μm). Upon increasing the magnification, the SEM images reveal that the particles are primarily aggregated and flocculated, with a tendency to form coated clusters. This uneven dispersion is a critical factor in understanding the material’s mechanical properties and failure mechanisms.

PMMA solution particles may flocculate after mixing and covering or during the tensile sample preparation heating process. The tensile samples have physical and thermal histories. At higher temperatures, the samples bubbled on the mold surface during the solvent evaporation in the vacuum oven. After removing the solvent, the dog bone mold samples were heated and compressed. Since the matrix molecules move during these heating processes, the particle migration and residence in the matrix may be possible.

Figure 9 provides a detailed SEM image of the PS- Al_2O_3 particles, showing their characteristics at different magnifications. At lower magnification (1.56 μm), the particles are clearly visible and exhibit a similar mass distribution.

Table 3. PS group tensile test properties

System	E (GPa)	σ_{ult} (MPa)	σ_y (MPa)	e_{ult}	e %
PS	3.7528	26.42	7.436	0.007282	0.7232
PS- Al_2O_3	3.2692	31.46	6.169	0.011760	1.1760

Table 4. Nanocomposite samples’ ultimate tensile strength and strain ranges

System	$\Delta\sigma_{ult}$	% $\Delta\sigma_{ult}$	e_{ult}	% Δe_{ult}
PPMA	38.22	--	0.01915	--
PMMA- Al_2O_3	44.52	16.483	0.02560	33.681
PS- Al_2O_3	31.46	19.0765	0.011760	61.49

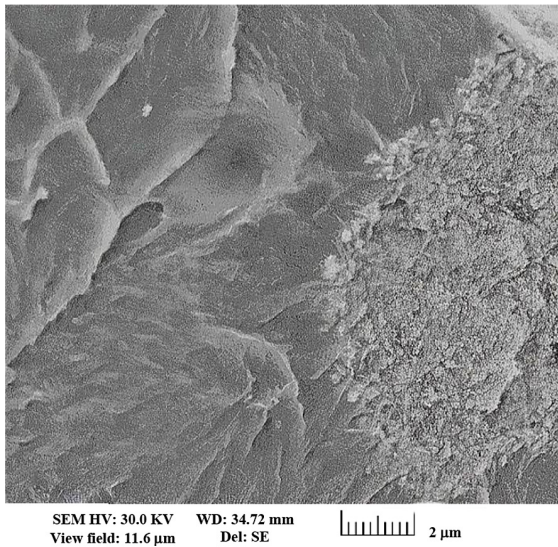


Figure 7. PMMA- Al_2O_3 SEM image of massive flocculants at low magnification

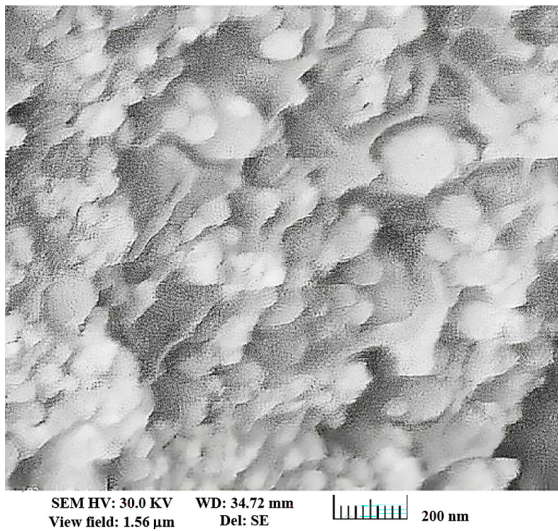


Figure 8. Close-up SEM of PMMA- Al_2O_3 flocculant particles

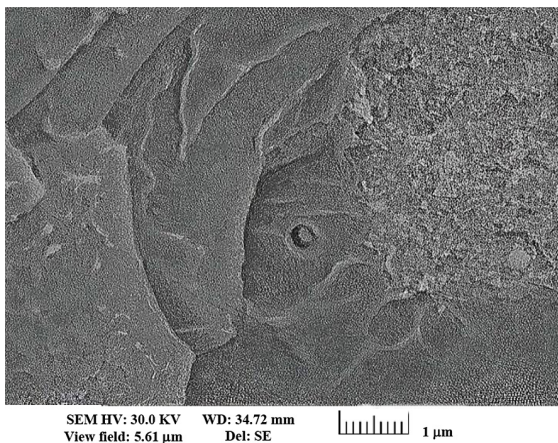


Figure 9. Low-magnification PS- Al_2O_3 SEM image showing particle dispersion

Upon increasing the magnification to $11.6 \mu\text{m}$, it becomes evident that the particles are well-separated, demonstrating a more uniform dispersion compared to other composites. The images consistently exhibit varying degrees of flocculation, with flocculants of different sizes present across the samples.

In contrast to the more uniform dispersion observed in the PS- Al_2O_3 composite, the PMMA- Al_2O_3 and PS- Al_2O_3 composites exhibit flocculants that are much larger, with diameters extending to several microns. The SEM scans further reveal that the dog bone-shaped samples, which are commonly used for tensile testing, contain regions where no visible particles are present. This absence of particles in certain areas may contribute to the observed heterogeneity in particle distribution, which could influence the final stress-strain behavior of the material. This heterogeneous dispersion pattern is important for understanding the material's mechanical properties, as it can explain some of the variations in stress and strain measurements observed during testing.

SEM images measure the particle size as the metal oxide cluster's diameter as well as the polymer's thickness of film attached to cluster. L_{eff} can be determined via computing the metal oxide clusters' diameter depending upon the reference data and the presumed geometry [9, 10]. This is a fundamental aspect of the suggested characterization approach. About 20 images of SEM were inspected for every sample; also, the all-detectable particles were measured upon every image. Since flocculants seemed to be covered with a polymer film, they were assessed separately. SEM VEGA3 offers the tools of measuring, which are applied

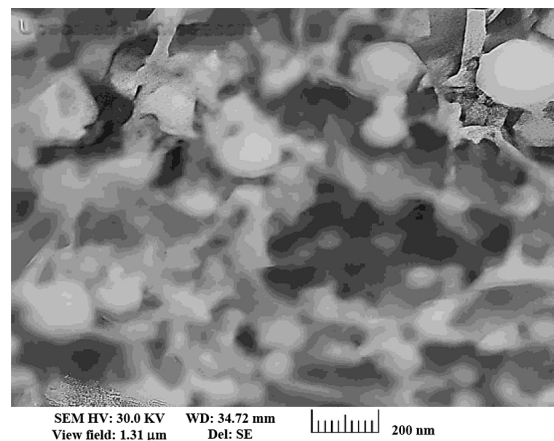


Figure 10. Close-up PS- Al_2O_3 SEM image of a tiny flocculant

to measure the particles size. Figures 11 and 12 depict an example for SEM pictures of the tested tensile specimen's fracture site for PMMA-Al₂O₃ and PS-Al₂O₃ correspondingly. Furthermore, such pictures show that the diameter of a particle can be calculated using the subsequent formula [13]:

$$d = \frac{2r}{Q_1} \times Q_{scale} \quad (1)$$

where: d – The diameter of particle, r – The radius of particle in the pixels, Q_1 – The scale measuring ruler's distance in the pixels, Q_{scale} – The scale of actual ruler.

By applying Equation 1 the diameter of PMMA-Al₂O₃ is computed.

$$d = \frac{2 \times 44}{94} \times 200 \text{ nm} = 187.234 \text{ nm} \quad (2)$$

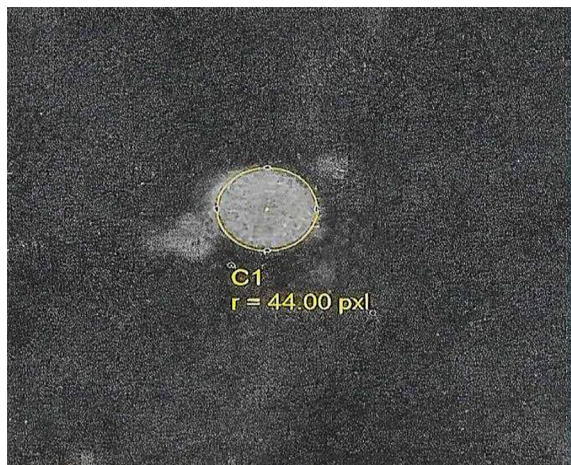


Figure 11. SEM image of the PMMA-Al₂O₃ tensile specimen fracture with measuring equipment

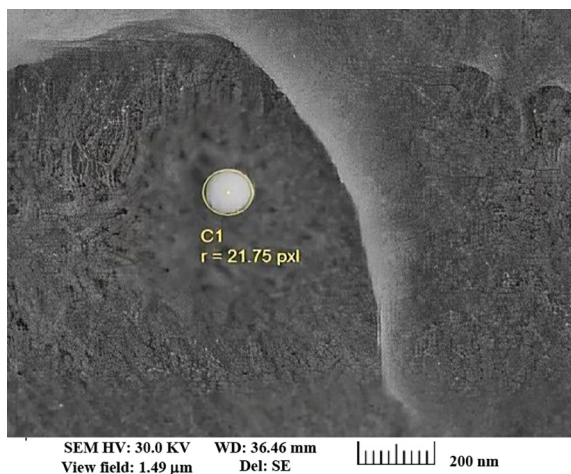


Figure 12. The image of PS-Al₂O₃ tensile specimen at the fracture with measuring equipment

Table 5. The calculated particle size (nm) based on SEM images

Particle size	PMMA-Al ₂ O ₃	PS-Al ₂ O ₃
Minimum measured diameter (nm)	138.0351	161.9022
Maximum measured diameter (nm)	245.3530	214.7137
Average diameter (nm)	201.117	184.6329
Standard deviation	32.4585	29.7534

All images were processed by the same way, as well as (20) particles were chosen for every tensile test specimen. Table 5 displays the mean of the whole (20) metrics.

A 20-measured diameter's minimum, maximum, and standard deviation are listed in this table. For both polymer system groups, the Al₂O₃ additive particle size changes with the different polymer matrices. Al₂O₃'s 110 nm initial particle size caused this disparity.

All systems have a wide particle size distribution due to bigger standard deviations. Some particles are below the manufacturer's starting diameter in all scanned images. Either this study's approach induced the separation of cluster or the produced particles possessed the size changes not stated in the chemical characteristics [16].

CONCLUSIONS

The purpose of this investigation is to determine the effect of Al₂O₃ nanoparticle additions on two pure polymer systems. Both of the manufactured systems (PMMA-Al₂O₃ and PS-Al₂O₃) are evaluated their mechanical properties and microstructure characteristics. The following conclusions can be drawn from the results of this study:

- The addition of 5 wt.% Al₂O₃ nanoparticles enhanced the mechanical properties of both PMMA and PS matrices.
- PMMA-Al₂O₃ nanocomposites showed an improvement of 16.5% in ultimate tensile strength (σ_{ult} , 44.52 MPa) and 33.7% in ultimate strain (ϵ_{ult} , 0.02560).
- PS-Al₂O₃ nanocomposites exhibited improvements of 19.1% in ultimate tensile strength (σ_{ult} , 31.46 MPa) and 61.5% in ultimate strain (ϵ_{ult} , 0.01176), compared to pure PS.
- SEM analysis revealed flocculation and uneven distribution of Al₂O₃ nanoparticles in both nanocomposite systems. At a low

magnification (1.56 μm), PS- Al_2O_3 nanoparticles were well-separated, while higher magnification (11.6 μm) revealed aggregation.

- The average nanoparticle diameters for PMMA- Al_2O_3 and PS- Al_2O_3 were 201.1 nm and 184.6 nm, respectively. Energy. The fracture areas of the dog bone samples displayed critical flocculation, indicating poor distribution.
- The blending technique employed for incorporating pre-formed nanoparticles into the polymer solution did not achieve optimal nanoparticle dispersion or size distribution.
- This technique lacked sufficient polymer-nanoparticle interaction, which is critical for improving dispersion and enhancing mechanical properties.
- Fracture surfaces of the dog bone samples indicated significant flocculation, confirming poor nanoparticle distribution and highlighting the need for more effective blending techniques.

REFERENCES

1. Salih, S. I., Oleiwi, J. K. and Mohamed A. S. Investigation of mechanical properties of PMMA composite reinforced with different types of natural powders, *ARNP Journal of Engineering and Applied Sciences*, 2018, 13(22), 8889–8900.
2. Merzah, Z. F., Fakhry, S., Allami, T. G., Yuhana, N. Y. and Alamiery, A. Enhancement of the properties of hybridizing epoxy and nanoclay for mechanical, industrial, and biomedical applications. *Polymers* 2022, 14(3), 526.
3. Shahrajabian, H., and Sadeghian, F. The investigation of alumina nanoparticles' effects on the mechanical and thermal properties of HDPE/rPET/MAPE blends. *International Nano Letters* 2019, 9(3), 213–219.
4. S. Zidan, N. Silikas, A. Alhotan, J. Haider, and J. Yates, "Investigating the mechanical properties of ZrO₂-impregnated PMMA nanocomposite for denture-based applications," *Materials*, Apr. 2019; 12(8), 1344, <https://doi.org/10.3390/ma12081344>
5. Jain, A. Tribology of carbon nanotubes/polymer nanocomposites, in *Tribology of Polymers, Polymer Composites, and Polymer Nanocomposites*, Elsevier, 2023, 195–214. <https://doi.org/10.1016/B978-0-323-90748-4.00003-0>
6. Din, S. H., Shah, M. A., Sheikh, N. A. and Butt M. M. Nano-composites and their applications: A review, *Characterization and Application of Nanomaterials*, Mar. 2020; 3(1), 40, <https://doi.org/10.24294/can.v3i1.875>
7. Omar, M. H., Amin, M. H. and Younis, H. A. Comparison of using nano-ZnO and nano- Al_2O_3 to improve the properties of prepared polymethyl methacrylate denture base, *Applied Physics A*, Apr. 2022, 128(4), 313, <https://doi.org/10.1007/s00339-022-05359-6>
8. Wu, C., Zhang, M., Rong M. and Friedrich, K. Tensile performance improvement of low nanoparticles filled-polypropylene composites, *Composites Science and Technology*, 2002, 62, 1327–1340.
9. Le, B., Khaliq, J., Huo, D., Teng, X. and Shyha, I. A review on nanocomposites. Part 1: mechanical properties. *Journal of Manufacturing Science and Engineering* 2020, 142(10), 100801.
10. Alam, S. N., Shrivastava, P., Ghosh, A., Sahoo, N., Shukla, U., Edara, A. C. and Ali, M. S. Fabrication Techniques Used for Nanofillers Based Materials. In *Handbook of Nanofillers*, Singapore: Springer Nature Singapore, 2024, 1–28.
11. Mohsin, M. K., Mustafa, A. M., Ahlatci, H. and Turen, Y. Mechanical behaviour for aluminum matrix anocomposites reinforced with single and dual nanoparticles ($\text{TiO}_2 + \text{SiO}_2$). In *AIP Conference Proceedings*, AIP Publishing, 2024, 3105(1).
12. Derazkola, H. A. and Simchi, A. Effects of alumina nanoparticles on the microstructure, strength and wear resistance of poly (methyl methacrylate)-based nanocomposites prepared by friction stir processing, *J Mech Behav Biomed Mater*, Mar. 2018, 79, 246–253, <https://doi.org/10.1016/j.jmbbm.2018.01.007>
13. Hussein, M. B., Mustafa, A. M., Abdulkareem, M. H. and Alamiery, A. Comparative corrosion performance of YSZ-coated Ti-13Zr-13Nb alloy and commercially pure titanium in orthopedic implants. *South African Journal of Chemical Engineering* 2024, 48(1), 40–54.
14. Mohsin, M. K., Mustafa, A., Ahlatci, H. and Turen, Y. Wear behaviour for aluminum matrix nanocomposites reinforced with ($\text{TiO}_2 + \text{SiO}_2$). In *AIP Conference Proceedings*, AIP Publishing, 2024, 3002(1).
15. Ahadzadeh, S. M., Hashimov, A. M. and Khalilova, S. G. Research of The Electrical Properties of Composite Varistors Based on ZnO-Polymer, *International Journal on Technical and Physical Problems of Engineering*, 2022, 14(1), 166–171.
16. Hashimov, A. M., Tabatabaei, N. M., Suleymanova, L. C., Taghiyeva, Z. A. and Gurbanov, K. B. Thermo-stimulating ionic currents in polymers in the environment of ozone gas, *International Journal on Technical and Physical Problems of Engineering*, 2019, 11(1), 21–24.
17. Krasinskyi, V., Suberlyak, O., Kochubei, V., Jachowicz, T., Dulebova, L. and Zemke, V. Nanocomposites based on polyamide and montmorillonite obtained from a solution. *Advances in Science and Technology. Research Journal* 2020, 14(3).